nature structural & molecular biology

Zika virus NS1 structure reveals diversity of electrostatic surfaces among flaviviruses

Hao Song[1,2], Jianxun Qi[1], Joel Haywood[1], Yi Shi[1–5] & George F Gao[1–6]

The association of Zika virus (ZIKV) infections with microcephaly has resulted in an ongoing public-health emergency. Here we report the crystal structure of a C-terminal fragment of ZIKV nonstructural protein 1 (NS1), a major host-interaction molecule that functions in flaviviral replication, pathogenesis and immune evasion. Comparison with West Nile and dengue virus NS1 structures reveals conserved features but diverse electrostatic characteristics at host-interaction interfaces, thus possibly implying different modes of flavivirus pathogenesis.

ZIKV, a Flaviviridae family member transmitted to humans by mosquitoes of the genus *Aedes*, was first isolated in Africa in 1947 (ref. 1) and has been found to commonly circulate in tropical regions in Africa and Asia[2]. After a large Zika outbreak in French Polynesia from 2013 to 2014, the virus was able to emerge into new territories of the American continent[3], and it has been found circulating in 26 countries and territories in South America and the Caribbean[4]. Before this outbreak, research on ZIKV pathogenesis was largely neglected because infected individuals are often asymptomatic or have mild symptoms. However there is now growing evidence that ZIKV infections may be linked to fetal and newborn microcephaly and serious neurological complications, such as Guillain–Barré syndrome[4]. ZIKV has been detected in the amniotic fluid of pregnant women whose fetuses had microcephaly syndrome and has also been detected in microcephalic fetal brain tissues[5,6]. Moreover, ZIKV infects human cortical neural progenitor cells and attenuates their growth[7]. Another matter of concern is that ZIKV may also be transmitted by sexual activity, and high viral loads have been detected in semen from infected patients[8]. To date, no clinically approved vaccines or therapeutics are available to prevent and control ZIKV infection. Given this urgent situation, great efforts are needed to develop new vaccines and antiviral therapeutics; to do so, a comprehensive understanding of the pathogenesis and molecular basis of ZIKV infection is required.

As a member of the Flaviviridae family, ZIKV has a single positive sense RNA genome, which is initially translated as a single polyprotein which is then cleaved post-translationally into three structural proteins (C, PrM or M, and E) and seven nonstructural (NS) proteins (NS1, NS2A, NS2B, NS3, NS4A, NS4B and NS5). Six of the NS proteins (NS2A to NS5) form a replication complex on the cytoplasmic side of the endoplasmic reticulum membrane. The glycosylated NS1, which associates with lipids, forms a homodimer inside the cells and is necessary for viral replication and late in infection[9]. NS1 is also secreted into the extracellular space as a hexameric lipoprotein particle[9], which is involved in immune evasion and pathogenesis by interacting with components from both the innate and adaptive immune systems, as well as other host factors[10,11]. NS1 is the major antigenic marker for viral infection[12], and it has been suggested, in combination with other markers, as a biomarker for early detection of dengue virus (DENV) infection[13]. The molecular mechanisms of NS1 are relatively well established for DENV and West Nile virus (WNV)[14,15], and the NS1-encoding sequence is suspected to be a major genetic factor underlying the diverse clinical consequences of infections caused by flaviviruses (over 70 members)[16,17]. However, little is known about the NS1 of ZIKV, which displays different pathogenesis from that of typical flaviviruses.

To address this lack of information, we expressed the ZIKV $NS1_{172–352}$ fragment of the BeH819015 strain isolated from Brazil in 2015 in

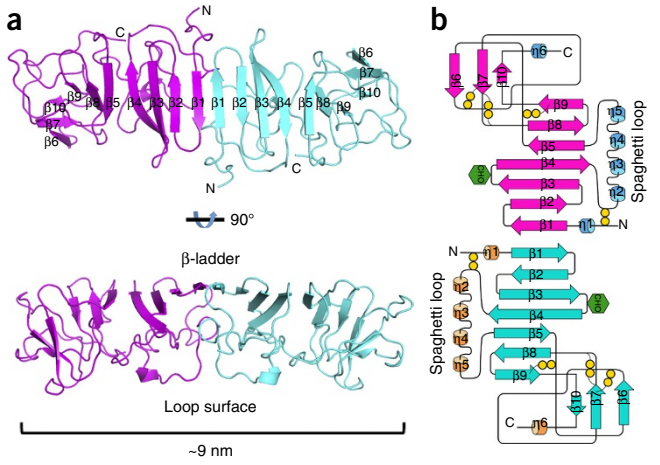

Figure 1 Overall structure of ZIKV $NS1_{172–352}$. (**a**) ZIKV $NS1_{172–352}$ forms a head-to-head dimer with one extended β-ladder platform and one loop surface on the opposite side. (**b**) Topology diagram for $NS1_{172–352}$. Glycosylation sites are indicated with green hexagons, and disulfide bonds are indicated with yellow circles. η represents the 3_{10} helix, and β represents the β-sheet.

[1]CAS Key Laboratory of Pathogenic Microbiology and Immunology, Institute of Microbiology, Chinese Academy of Sciences, Beijing, China. [2]Research Network of Immunity and Health (RNIH), Beijing Institutes of Life Science, Chinese Academy of Sciences, Beijing, China. [3]Shenzhen Key Laboratory of Pathogen and Immunity, Shenzhen Third People's Hospital, Shenzhen, China. [4]Center for Influenza Research and Early-warning (CASCIRE), Chinese Academy of Sciences, Beijing, China. [5]Savaid Medical School, University of Chinese Academy of Sciences, Beijing, China. [6]National Institute for Viral Disease Control and Prevention, Chinese Center for Disease Control and Prevention (China CDC), Beijing, China. Correspondence should be addressed to G.F.G. (gaof@im.ac.cn) or Y.S. (shiyi@im.ac.cn).

Received 11 March; accepted 25 March; published online 18 April 2016; doi:10.1038/nsmb.3213

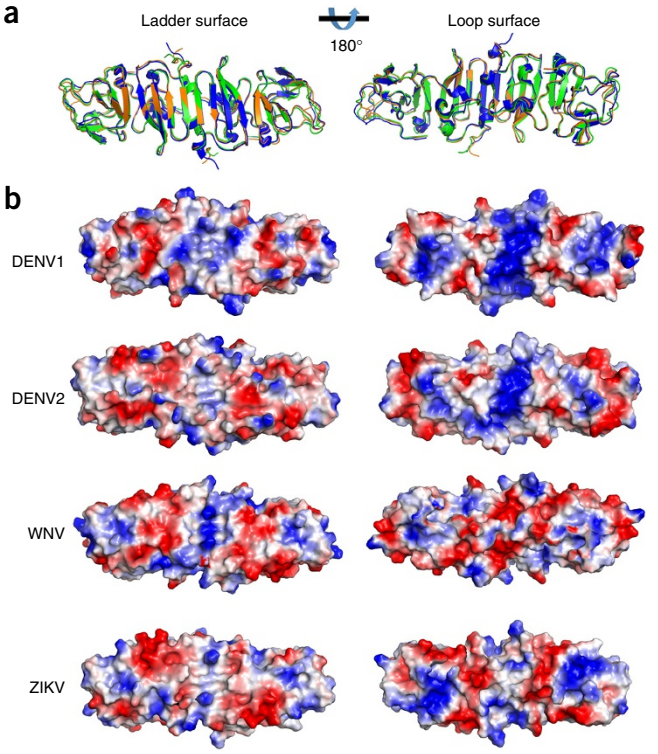

Figure 2 Comparison of ZIKV $NS1_{172–352}$ with other known $NS1_{172–352}$ structures. (**a**) Superimposed structures in ribbon representation of NS1 from ZIKV (orange), dengue virus type 1 (DENV1, blue), dengue virus type 2 (DENV2, green) and West Nile virus (WNV, magenta). (**b**) Electrostatic surface views of the same four $NS1_{172–352}$ structures, showing common features on the β-ladder face but diverse characteristics on the loop surface.

Escherichia coli as inclusion bodies and obtained the soluble protein by *in vitro* refolding (Online Methods). We then solved its crystal structure by molecular replacement to a resolution of 2.2 Å (R_{work} and R_{free} values of 0.205 and 0.246, respectively) (**Supplementary Table 1**). The ZIKV $NS1_{172–352}$ protein crystallized as a rod-like homodimer with a length of ~9 nm (**Fig. 1a**). Sedimentation velocity analytical ultracentrifugation analyses confirmed that the ZIKV $NS1_{172–352}$ protein exists as a homodimer (~40 kDa) in solution (**Supplementary Fig. 1**).

The ZIKV $NS1_{172–352}$ homodimer structure has a continuous β-sheet on one surface, with 20 β-strands arranged like the rungs of a ladder (**Fig. 1a**), in which each monomer contributes ten rungs to the antiparallel β-ladder. On the opposite side of the homodimer, an irregular surface is formed by a complex arrangement of loop structures (**Fig. 1a**). Most of those interstrand loops are short, except for a long 'spaghetti loop' between β4 and β5 that lacks secondary structure (**Fig. 1a**,**b**). A potential N-linked glycosylation site that is highly conserved in the Flaviviridae family is located in the β3–β4 loop (**Fig. 1b**).

We built a phylogenetic tree by using the ZIKV NS1 protein sequence and those of ten other flaviviruses—WNV, DENV types 1 to 4 (DENV1–4), Japanese encephalitis virus (JEV), St. Louis encephalitis virus (SLEV), yellow fever virus (YFV), Murray Valley encephalitis virus (MVEV) and tick-borne encephalitis virus (TBEV) (**Supplementary Fig. 2**). This analysis revealed that these flaviviruses can be classified into four groups on the basis of their NS1 sequences: the DENV group (DENV1–4), the WNV group (WNV, JEV, SLEV and MVEV), the YFV group (YFV and TBEV) and an independent ZIKV group. This result suggests that different flaviviruses may have group-specific NS1 characteristics and that the ZIKV NS1 may have properties that are unique among the four groups.

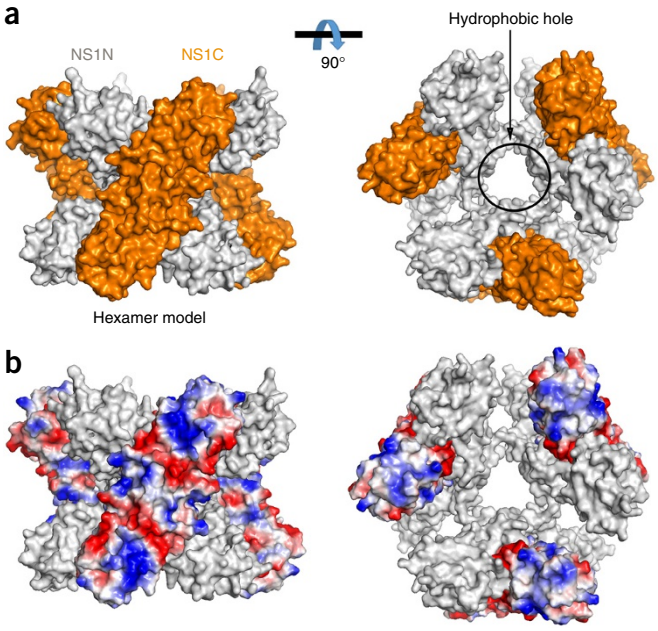

We compared the ZIKV $NS1_{172–352}$ structure with the available NS1 structures of DENV1, DENV2 and WNV (**Fig. 2**). ZIKV $NS1_{172–352}$ is structurally similar to the aforementioned NS1 structures (**Fig. 2a**), despite having protein sequence identities in the range of 53–56%. Interestingly, the electrostatic surface potential maps of these proteins show several group-specific features in the loop surface (**Fig. 2b**). The DENV1 and DENV2 NS1 structures both display a positively charged surface in the central regions of their loop surfaces, whereas the WNV NS1 structure has a negatively charged central region in its loop surface. For ZIKV, the loop surface exhibits a composite platform containing both a positively and negatively charged central region and a negative charge toward the two distal ends.

The similarities between the NS1 structures of ZIKV and DENV2 allowed us to create a ZIKV NS1 hexamer model (**Supplementary Data Set 1**) based on the DENV2 NS1 hexamer structure (PDB 4O6B)[14]. The ZIKV NS1 model shows a hexameric arrangement of three dimers forming a symmetric barrel shape (**Fig. 3a**). In the center of the barrel, a hydrophobic hole could easily accommodate host lipids to form a complex lipoprotein. In this model, the loop surface of $NS1_{172–352}$ is fully exposed, facing outward, while the β-ladder surface faces inward (**Fig. 3b**).

The loop surface has been suggested to play a crucial role in interactions of secreted NS1 hexamers with host factors and antibodies[15,18]. Furthermore, antibodies to DENV NS1 have been implicated in immune pathogenesis[16,19], and epitopes of antibodies with cross-reactivity to human proteins have been mapped to the conserved tip (residues 311–330) of $NS1_{172–352}$ (**Supplementary Fig. 3**). Within this

Figure 3 Model of the ZIKV NS1 hexamer. (**a**) The ZIKV NS1 hexamer, modeled by using the full-length DENV2 NS1 structure (PDB 4O6B)[14]. The actual $NS1_{172–352}$ structure is colored in orange, and the predicted $NS1_{1–171}$ structure is colored in light gray. $NS1_{172–352}$ is located in the outer layer of the hexamer barrel. (**b**) Electrostatic presentation of the $NS1_{172–352}$ structure in the hexamer model.

conserved tip, ZIKV NS1 has a negatively charged residue Glu315, which is not present in our sequence alignment with ten other flaviviruses (**Supplementary Fig. 3**).

In summary, our study describes the crystal structure of a C-terminal fragment of ZIKV NS1. Despite having high structural similarity with other flavivirus NS1 proteins, ZIKV NS1 displays a loop-surface interface with divergent electrostatic potential that may result in altered binding properties to host factors and to known protective antibodies to flavivirus NS1; this possibility should be further studied in the near future. Eliciting such antibodies is considered to be an attractive approach in vaccine development, because they would circumvent the enhancement of infection associated with anti-envelope antibodies in DENV[13]. The unique surface electrostatic potentials in the three known flavivirus NS1 structures (for DENV, WNV and ZIKV) provide a new direction for future studies of more NS1 structures of flavivirus members with diverse clinical outcomes. The unique surface characteristics of ZIKV NS1 may be exploited in the development of new diagnostic tools for ZIKV infection. These future studies may elucidate a clearer scenario of the role that NS1 plays in flavivirus pathogenesis.

METHODS

Methods and any associated references are available in the online version of the paper.

Accession codes. Coordinates and structure factors have been deposited in the Protein Data Bank under accession code PDB 5IY3.

Note: Any Supplementary Information and Source Data files are available in the online version of the paper.

ACKNOWLEDGMENTS

This work was supported by the Emergency Task-Force Project (grant no. 81641001) of the National Natural Science Foundation of China (NSFC), the China Ministry of Science and Technology National 973 Project (grant no. 2015CB910500) and the Task Force of Zika Virus Research from the Chinese Academy of Sciences (CAS) and the Zika Special Project of the National Infectious Disease Control S&T Grand Project and Strategic Priority Research Program of the CAS (XDB08020100).

We thank the staff of the BL17U beamline at the Shanghai Synchrotron Radiation Facility for assistance during data collection. We thank X. Xu, H. Wang and Z. Su for assistance in protein preparation. Y.S. is supported by the Excellent Young Scientist Program of the CAS and the Youth Innovation Promotion Association, CAS (2015078). G.F.G. is supported partly as a leading principal investigator of the NSFC Innovative Research Group (grant no. 81321063).

AUTHOR CONTRIBUTIONS

G.F.G. and Y.S. designed and supervised the study. H.S. conducted the experiments. J.Q. collected the data sets and solved the structures. Y.S., J.H., H.S. and G.F.G. analyzed the data and wrote the manuscript.

COMPETING FINANCIAL INTERESTS

The authors declare no competing financial interests.

1. Dick, G.W., Kitchen, S.F. & Haddow, A.J. *Trans. R. Soc. Trop. Med. Hyg.* **46**, 509–520 (1952).
2. Faye, O. *et al. PLoS Negl. Trop. Dis.* **8**, e2636 (2014).
3. Cao-Lormeau, V.M. & Musso, D. *Lancet* **384**, 1571–1572 (2014).
4. Petersen, E. *et al. Int. J. Infect. Dis.* **44**, 11–15 (2016).
5. Calvet, G. *et al. Lancet Infect. Dis.* http://dx.doi.org/10.1016/S1473-3099(16)00095-5 (2016).
6. Mlakar, J. *et al. N. Engl. J. Med.* **374**, 951–958 (2016).
7. Tang, H. *et al. Cell Stem Cell* http://dx.doi.org/10.1016/j.stem.2016.02.016 (2016).
8. Mansuy, J.M. *et al. Lancet Infect. Dis.* http://dx.doi.org/10.1016/S1473-3099(16)00138-9 (2016).
9. Suthar, M.S., Diamond, M.S. & Gale, M. Jr. *Nat. Rev. Microbiol.* **11**, 115–128 (2013).
10. Avirutnan, P. *et al. J. Exp. Med.* **207**, 793–806 (2010).
11. Chung, K.M. *et al. Proc. Natl. Acad. Sci. USA* **103**, 19111–19116 (2006).
12. Young, P.R., Hilditch, P.A., Bletchly, C. & Halloran, W. *J. Clin. Microbiol.* **38**, 1053–1057 (2000).
13. Muller, D.A. & Young, P.R. *Antiviral Res.* **98**, 192–208 (2013).
14. Akey, D.L. *et al. Science* **343**, 881–885 (2014).
15. Edeling, M.A., Diamond, M.S. & Fremont, D.H. *Proc. Natl. Acad. Sci. USA* **111**, 4285–4290 (2014).
16. Cheng, H.J. *et al. Exp. Biol. Med. (Maywood)* **234**, 63–73 (2009).
17. Kuno, G., Chang, G.J., Tsuchiya, K.R., Karabatsos, N. & Cropp, C.B. *J. Virol.* **72**, 73–83 (1998).
18. Avirutnan, P. *et al. PLoS Pathog.* **3**, e183 (2007).
19. Liu, I.J., Chiu, C.Y., Chen, Y.C. & Wu, H.C. *J. Biol. Chem.* **286**, 9726–9736 (2011).

ONLINE METHODS

Gene cloning, protein expression and purification. Coding-sequence-optimized synthetic DNA encoding the ZIKV NS1 C-terminal region (amino acids 172–352, GenBank AMA12085) was cloned into the pET-21a vector (Novagen) with NdeI and XhoI restriction sites and was transformed into *Escherichia coli* strain BL21(DE3) for protein expression. The inclusion bodies of recombinant proteins were purified and then refolded as previously described, by gradual dilution of the inclusion bodies in a refolding buffer (100 mM Tris-HCl, 2 mM EDTA, 400 mM L-arginine, 0.5 mM oxidized glutathione and 5 mM reduced glutathione, pH 8.0) at 4 °C. The refolded protein was concentrated and purified by gel-filtration chromatography in a buffer containing 20 mM Tris-HCl and 50 mM NaCl, pH 8.0, on a HiLoad 16/60 Superdex 200 PG column (GE Healthcare) and then was further purified by ion-exchange chromatography with a 6-ml RESOURCE Q column (GE Healthcare). For crystallization, the proteins were further purified by gel-filtration chromatography with a Superdex 75 10/300 GL column (GE Healthcare) with a running buffer of 20 mM Tris-HCl and 50 mM NaCl, pH 8.0, and the collected protein fractions were concentrated to 10 mg/mL with a membrane concentrator with a molecular-weight cutoff of 10 kDa (Millipore).

Crystallization, data collection and structure determination. The initial screening trials were set up with commercial crystallization kits (Molecular Dimensions) with the sitting-drop vapor-diffusion method. Typically, 1 µL protein (5 or 10 mg/mL in 20 mM Tris, pH 8.0, and 50 mM NaCl) was mixed with 1 µL reservoir solution. The resultant drop was then sealed and equilibrated against 100 µL reservoir solution at 4 or 18 °C. Diffractable crystals were obtained in a reservoir solution containing 0.03 M $NaNO_3$, 0.03 M Na_2HPO_4, 0.03 M $(NH_4)_2SO_4$, 0.1 M buffer mix, pH 6.5 (44.5 mM imidazole, pH 10.23, and 55.5 mM MES, pH 3.11), 12.5% MPD, 12.5% PEG 1000 and 12.5% PEG 3350. Crystals were flash-cooled in liquid nitrogen after briefly being soaked in reservoir solution with 17% (v/v) glycerol added. The X-ray diffraction data were collected under cryogenic conditions (100 K) at a wavelength of 0.97915 Å at the Shanghai Synchrotron Radiation Facility (SSRF) beamline BL17U and were indexed, integrated and scaled with HKL2000 (ref. 20).

The ZIKV $NS1_{172–352}$ structure was solved by the molecular replacement method with Phaser[21] from the CCP4 program suite[22], with the structure of DENV2 $NS1_{172–352}$ (PDB 4OIG) as the search model. Initial restrained rigid-body refinement and manual model building were performed with REFMAC5 (ref. 23) and COOT[24], respectively. Further refinement was performed with Phenix[25]. In the final Ramachandran plot, 93.43% and 99.43% of residues were in the favored and allowed regions, respectively. The final statistics for data collection and structure refinement are shown in **Supplementary Table 1**.

Modeling of ZIKV NS1 hexamer. The structural model of ZIKV $NS1_{1–171}$ was built with the SWISS-MODEL online server (http://www.swissmodel.expasy.org/). The crystal structure of DENV2 NS1 (PDB 4O6B) was used as a template to build the model. The hexamer structural model of ZIKV NS1 was constructed by superimposing the ZIKV $NS1_{1–171}$ model and the ZIKV $NS1_{172–352}$ crystal structure with the DENV2 NS1 hexamer structure (PDB 4O6B). The coordinate file for this model is provided as **Supplementary Data Set 1**.

Biochemical characterization of the protein. The purified protein was analyzed with an analytical gel-filtration assay with a calibrated Superdex 75 10/300 GL column (GE Healthcare). The samples were further analyzed with SDS–PAGE.

The analytical ultracentrifugation assay was performed according to a previously reported method[26]. The proteins were prepared in 20 mM Tris, pH 8.0, and 50 mM NaCl at a concentration of $A_{280} = 0.8$. The assay was performed on an optimal XL-I analytical ultracentrifuge (Beckman Coulter) at a speed of 60,000 r.p.m.

20. Otwinowski, Z. & Minor, W. *Methods Enzymol.* **276**, 307–326 (1997).
21. Read, R.J. *Acta Crystallogr. D Biol. Crystallogr.* **57**, 1373–1382 (2001).
22. Collaborative Computational Project, Number 4. *Acta Crystallogr. D Biol. Crystallogr.* **50**, 760–763 (1994).
23. Murshudov, G.N., Vagin, A.A. & Dodson, E.J. *Acta Crystallogr. D Biol. Crystallogr.* **53**, 240–255 (1997).
24. Emsley, P. & Cowtan, K. *Acta Crystallogr. D Biol. Crystallogr.* **60**, 2126–2132 (2004).
25. Adams, P.D. *et al. Acta Crystallogr. D Biol. Crystallogr.* **66**, 213–221 (2010).
26. Zhang, N. *et al. Nat. Commun.* **2**, 577 (2011).